

Unsaturated polyester resin/epoxy-functionalised nanosilica composites constructed by *in situ* polymerisation

Haiyang Yao¹, Hao Pan¹, Rui Rui Li¹, Xiaohong Li^{1,2}, Zhijun Zhang^{1,2}

¹Key Laboratory of Ministry of Education for Special Functional Materials, Henan University, Kaifeng 475004, Henan Province, People's Republic of China

²Collaborative Innovation Center of Nano Functional Materials and Applications, Henan University, Kaifeng 475004, Henan Province, People's Republic of China

E-mail: xiaohonglihenu@126.com

Published in Micro & Nano Letters; Received on 6th March 2015; Revised on 19th May 2015; Accepted on 22nd May 2015

A reactable nanosilica surface capped with a silane coupling agent containing the epoxy group (denoted as RNS-E) was allowed to participate in the *in situ* polycondensation reaction of unsaturated polyester resin (denoted as UPR) thereby affording the UPR/RNS-E composite. The structure of the as-prepared UPR/RNS-E composites was investigated by means of Fourier transform infrared spectrometry, thermogravimetric analysis and scanning electron microscopy, and their tensile strength and impact strength were compared with those of pure UPR cured under the same condition and of UPR/RNS-E composites prepared by mechanical blending. It was found that RNS-E exhibits good strengthening effect and toughening effect for the *in situ* polymerised UPR/RNS-E composite, which is attributed to the formation of a heterogeneous network structure in the cured UPR/RNS-E composites via the chemical reaction among the epoxy group of RNS-E and the hydroxyl (carboxyl) group of UPR. Particularly, the UPR/RNS-E composite with 0.6% RNS-E nanofiller has the highest tensile strength and impact strength, and it is much superior to the same composite obtained by mechanical blending.

1. Introduction: Unsaturated polyester resin (denoted as UPR), one of the most widely used thermosetting resins, exhibits low cost and low density as well as high corrosion resistance and good processability [1, 2]. However, the pure UPR has some drawbacks such as polymerisation shrinkage, inherent brittleness and low resistance to crack propagation because of the high degree of cross-linking, which limits its application in engineering [3–5]. To overcome these shortcomings, many researchers have made tremendous efforts to improve the comprehensive performance of UPR through incorporating various inorganic fillers. Of the various inorganic fillers, inorganic nanoparticles with the ability to significantly enhance the mechanical properties of UPR are of particular significance [6], and nanosilica with its high surface activity and rigidity as well as good dimensional stability is of particular interest [7].

Naturally, the uniform dispersion of nanofillers throughout polymer matrices is critical to maximise the interaction between the intermixed phases [8]. The conventional mechanical blending method, however, is usually inapplicable to acquire the uniform dispersion of nanoparticles in polymer matrices, largely because of the weak interaction between the nanoparticles and polymeric matrices and because of the susceptibility to agglomeration of the nanoparticles at an increased dosage [9]. In this respect, *in situ* polymerisation, characterised by the direct synthesis of polymer-matrix composites ‘via’ polycondensation in the presence of nanofillers and organic monomers, is more competitive than the conventional mechanical blending method. Actually, *in situ* polymerisation is considered as the most powerful technique to produce polymer-matrix composites containing well distributed and dispersed nanoscale fillers [10, 11], and its use in fabricating novel polymer-matrix composites could be further promoted by simultaneously applying surface modification of the nanofillers. This is because the active functional groups of the surface-capping agent can readily react with highly active hydroxyl groups on the surface of inorganic nanoparticles, thereby preventing them from agglomeration [12]. However, the conventional modification of nanosilica powder by surface capping of the coupling agent is not so effective as expected in improving the dispersion of nanosilica, which is because the

hydroxyl group and the unsaturated dangling bond of nanosilica are extremely active and tend to be deactivated and saturated on the exposure of silica (SiO₂) to air. As a result, the chemical reaction between the active functional groups of the coupling agents and the active groups of SiO₂ is retarded, thereby leading to a low surface-modifying efficiency for nanosilica [13].

In view of the above-mentioned perspectives, we anticipate that the compatibility of nanosilica with the polymer matrix and its dispersion therein could be significantly improved by combining *in situ* polymerisation with *in situ* surface modification of nanosilica. Therefore, in our previous work, we synthesised a series of reactable nano SiO₂ (coded as RNS) by means of *in situ* surface modification [13, 14], and in this present Letter, we adopt a chosen RNS surface capped with a silane coupling agent containing the epoxy group (denoted as RNS-E) as a reaction monomer to directly take part in the polycondensation reaction of UPR, thereby yielding UPR/RNS-E composites via *in situ* polymerisation based on the reaction among the epoxy group of RNS-E and the carboxyl and hydroxyl groups of UPR. This Letter reports on the preparation of UPR/RNS-E composites as well as on the valuation of their mechanical properties.

2. Experimental

2.1. Materials: RNS-E was prepared with the method established in our laboratory [13, 14], and the as-obtained RNS-E is of spherical shape and has an average diameter of 25 nm and a specific surface area of 100 ± 20 m²/g (as shown in Fig. 1). Fig. 2 schematically illustrates the processes for the fabrication of RNS-E. Briefly, RNS-E is fabricated through a condensation-like polymerisation associated with *in situ* surface modification in the presence of sodium metasilicate as the source of silicon and silane coupling agent KH560 as the surface-capping agent. Namely, sodium metasilicate is hydrolysed to generate the silicic acid (Si(OH)₄) monomer. The resultant Si(OH)₄ monomer undergoes condensation polymerisation to afford silica spheres containing active hydroxyl group on the surface. On the introduction of the KH560 silane coupling agent, chemical reaction occurs between the condensation product and the silane coupling agent (the chain

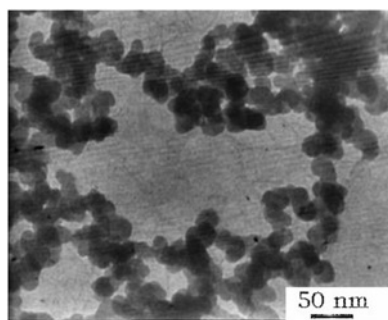


Figure 1 TEM images of RNS-E

terminator) to afford RNS-E containing both hydroxyl and epoxy active groups.

Industrial grade reagents include phthalic anhydride, maleic anhydride, propylene glycol, styrene and paraffin. Photographic grade hydroquinone and analytical grade reagents including concentrated sulphuric acid, sodium hydroxide, potassium hydroxide, anhydrous ethanol and acetone which were obtained from commercial sources.

2.2. Preparation of UPR/RNS-E composites: UPR/RNS-E composites were prepared through the polycondensation of maleic anhydride, phthalic anhydride and propylene glycol (molar ratio 1:1:2.2) in the presence of a proper amount of RNS-E filler. The polycondensation reaction was conducted in a three-necked flask equipped with a Dean-Stark trap. Briefly, the reactants were heated to 160°C in about 1.5 h, followed by gradual heating to 200°C and holding there until the acid value declined to 80 mg potassium hydroxide (KOH)/g. The resultant reaction system was maintained under gradually elevated vacuum pressure till the acid value dropped to 40 mg KOH/g on the completion of heating. When the temperature of the reaction system was decreased to 110°C, the styrene monomer was added at a mass fraction of 35% to the polycondensation product and hydroquinone as the inhibitor was added at a mass fraction of 0.1% to avoid polymerisation of the prepolymer. Into 100 g of resultant primary polycondensation product were added 1 g of cobalt naphthenate and 2 g of methyl-ethyl ketone peroxide under magnetic stirring to initiate the curing process. On completion of the curing process, the final target products, cured UPR/RNS-E composites, were obtained.

2.3. Characterisation: A proper amount of the uncured UPR/RNS-E composite was dissolved in acetone and centrifuged at 3000 min^{-1} to extract the nanosilica particulates. After the supernatant liquid was removed, the remnant precipitate was washed with acetone and centrifuged again. The above procedures were repeated until no free polyester chain was detected in the supernatant liquid (the contents of carboxyl were detected by sodium hydroxide

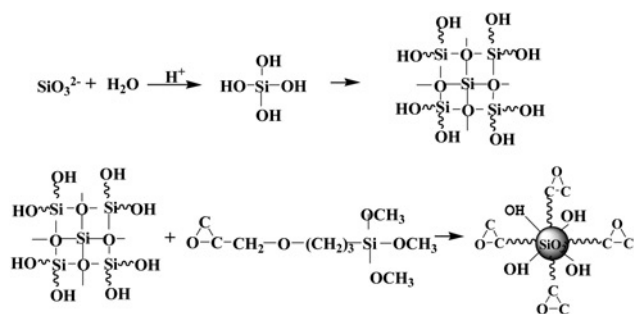


Figure 2 Schematic diagram illustrating formation of RNS-E

titration). The centrifuged precipitate (denoted as C-RNS) was dried in air. RNS-E and C-RNS were pressed into potassium bromide pellets, and their Fourier transform infrared (FT-IR) spectra were recorded with an AVATAR360 FT-IR spectrometer (Nicolet Corporation, USA). Thermogravimetric analyses (TGA) of RNS-E and C-RNS in nitrogen atmosphere were conducted using an EXSTAR 6000 thermal analysis system (Seiko Instruments Inc., Japan) in the temperature range of 20–1000°C at a heating rate of 10°C min^{-1} . The tensile strength of the cured composite (size: 10 × 200 × 4 mm^3) was measured with an electronic tensile testing equipment (WDW-10D, Jinan Shijin Testing Machine Group Company, Jinan, China) at a tensile rate of 10 $\text{mm} \cdot \text{min}^{-1}$ in accordance with the Chinese National Standard Method GB/T2567-2008. The impact strength of the cured composite specimen (size: 80 × 10 × 4 mm^3) was determined with a pendulum impact tester (XC-2.75D, Shenzhen Xinsansi Materials Testing Co. Ltd. Shenzhen, China) at a velocity of 2.9 ms^{-1} and an impact pendulum angle of 160° in accordance with the Chinese National Standard Method GB/T2567-2008. The morphologies of the fractured surface of the *in situ* polymerised UPR/RNS-E composites were observed with a scanning electron microscope (SEM) (model 6360, JEOL, Japan).

3. Results and discussion of RNS-E and C-RNS

3.1. FT-IR and TGA analyses: Fig. 3 shows the FT-IR spectra of RNS-E and C-RNS. The absorption peaks at 471, 801 and 1107 cm^{-1} correspond to the bending vibration, symmetric stretching vibration and asymmetric stretching vibration of Si–O–Si, respectively. The absorption bands at 1631 and 3426 cm^{-1} correspond to the bending vibration and stretching vibration of –OH [15, 16]. Particularly, the –OH stretching vibration peaks in curve *b* are much stronger than those in curve *a*, which prove that chemical bonding occurs between the RNS-E filler and the UPR matrix. Such a chemical bonding is also supported by the fact that the stretching vibration peak of ester carbonyl (C=O) at 1730 cm^{-1} is still retained as seen from Fig. 3*a* even after the C-RNS is repeatedly washed with acetone to remove unsaturated polyester chains. Furthermore, the C-RNS shows the absorption peaks of 1,2-disubstituted orthophthalic species in the range of 742–709 cm^{-1} [17], but it does not retain the asymmetric stretching vibration peaks of the epoxide ring in the range of 913–945 cm^{-1} as well as the stretching vibration peak of C–O in the epoxide ring at 914 cm^{-1} , which confirms that the epoxy group of RNS-E chemically reacts with the hydroxyl group or the carboxyl group of the unsaturated polyester [18]. On the basis of these FT-IR data, it can be supposed that the unsaturated polyester chains mainly combined with the RNS-E by chemical bonding rather than by physical adsorption.

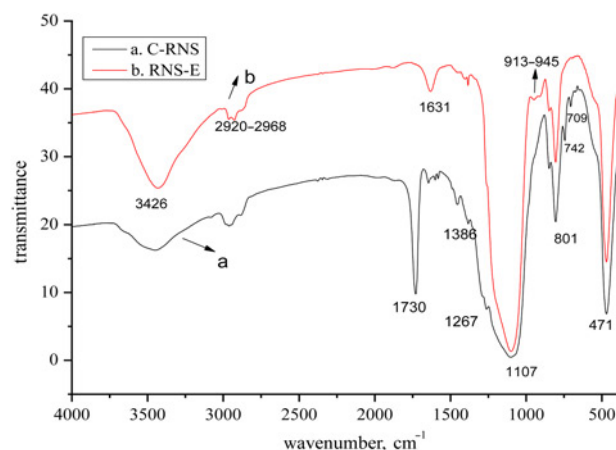


Figure 3 FT-IR spectra of RNS-E and C-RNS

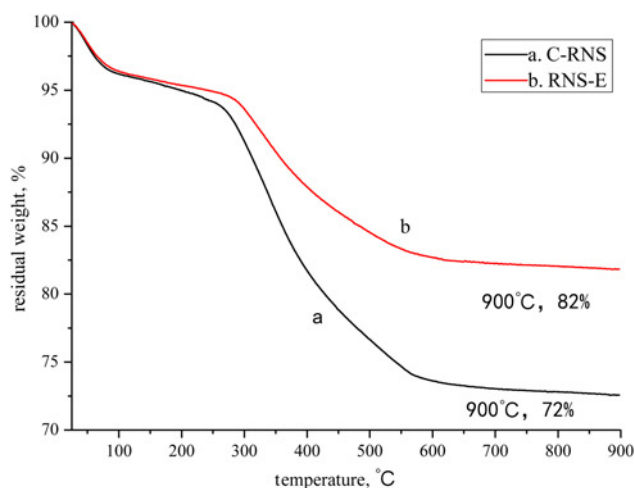


Figure 4 TGA thermograms of RNS-E and C-RNS

The TGA curves of RNS-E and C-RNS are given in Fig. 4. It can be seen that RNS-E and C-RNS have the same weight loss of 3% in the temperature range of 0–200°C, which is because of the volatilisation of absorbed water. Their weight loss in the range of 200–600°C is because of the decomposition and breakage of the organic carbon chain on the surface of the silica [19]; C-RNS exhibits a much higher weight loss (28%) than RNS-E (18%) in this range of temperature, which indicates that the former contains a higher mass fraction of the organic carbon chain than the latter. Moreover, C-RNS even experiences a slight weight loss from 600 to 680°C, possibly because of dehydration condensation via surface residual hydroxyls.

The above-mentioned FT-IR and TGA data demonstrate that RNS-E participates in the polycondensation reaction of the unsaturated polyester matrix; the reaction between RNS-E and the unsaturated polyester chains can be schematically illustrated as in Fig. 5. During the condensation stage of the unsaturated polyester, the carboxyl and hydroxyl groups of the polyester chains can chemically react with the epoxy group of RNS-E thereby forming covalent bonds. Namely, the carboxyl can attack and open the epoxy bond to form ester bonds in association with the hydroxyl group at the other end of the opened epoxy bond (Fig. 5a); in the meantime, the hydroxyl can attack and open the epoxy bond to form an ether bond in association with the hydroxyl group at the other end of the epoxy bond (Fig. 5b).

3.2. Mechanical properties of UPR/RNS-E composite: The impact strength and tensile strength of *in situ* polymerised UPR/RNS-E composites containing different contents of RNS-E are shown in

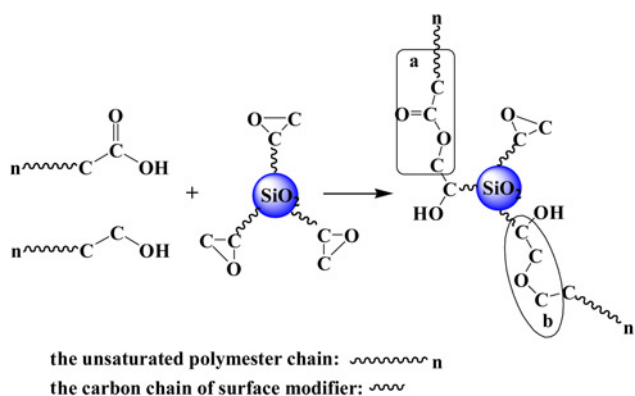


Figure 5 Schematic diagram illustrating the reaction between RNS-E and unsaturated polyester chain

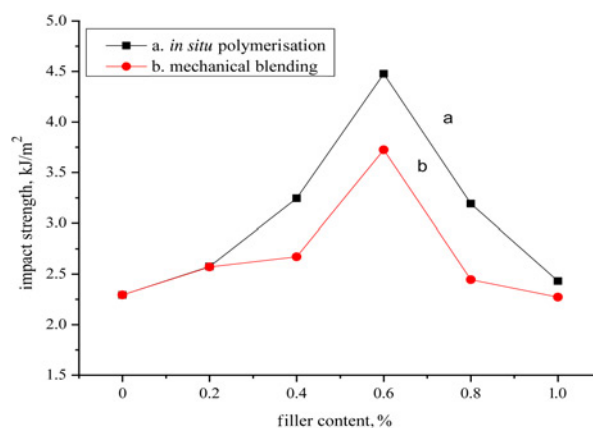


Figure 6 Impact strength of cured UPR/RNS-E composites

Figs. 6 and 7, respectively, where these composites prepared by mechanical blending are also presented for comparison. It is seen that the impact strength of UPR/RNS-E composites prepared by *in situ* polymerisation and mechanical blending gradually rises with increasing RNS-E dosage below 0.6%, and their impact strength reaches the maximum when the RNS-E dosage reaches 0.6%. As the dosage of RNS-E is above 0.6% (0.8 and 1.0%), the impact strength of the composites tends to decline to some extent with increasing filler content. Moreover, *in situ* polymerised UPR/RNS-E composites containing different contents of RNS-E exhibit slightly higher impact strength than the one prepared by mechanical blending, which is because *in situ* polycondensation is favourable for improving the compatibility between the polymer matrix and the inorganic filler and enhancing their interfacial interaction. The introduction of RNS-E at a dosage below 0.6% leads to a gradual increase in tensile strength of the *in situ* polymerised UPR/RNS-E composites, and the reinforcing effect of RNS-E for the *in situ* UPR/RNS-E composite tends to decline slightly as the dosage of RNS-E is above 0.6% (0.8 and 1.0%), which is possibly because the nanoscale filler is more liable to the aggregation threat. Furthermore, as the filler content is above 0.2%, the UPR/RNS-E composites prepared by the mechanical blending method even exhibit much lower tensile strength than the pure UPR, which is because RNS-E with a relatively high level of dosage (above 0.2% in this Letter) cannot be homogeneously dispersed in the UPR matrix by mechanical blending [20].

During the *in situ* polymerisation process, RNS-E can be well dispersed in the polymer matrix, because of its improved compatibility with polyester chains. The epoxy group on the surface of

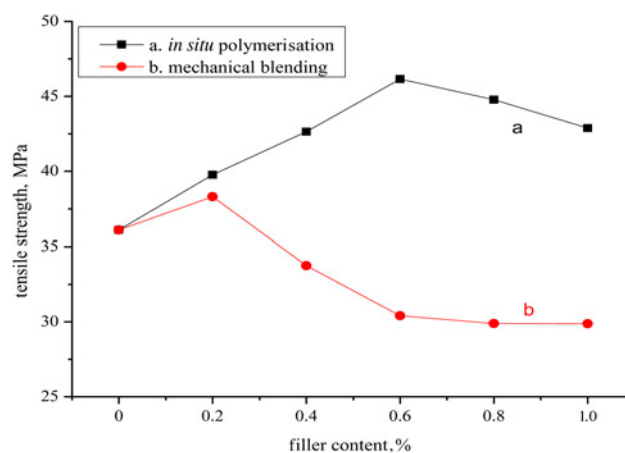


Figure 7 Tensile strength of cured UPR/RNS-E composites

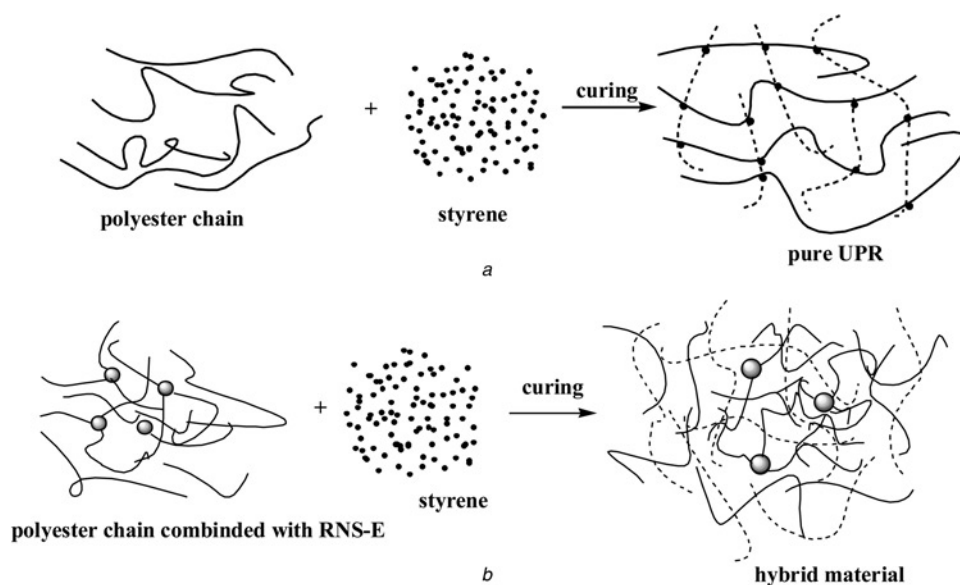


Figure 8 Schematic diagram illustrating curing process of pure UPR and UPR/RNS-E composite

a UPR

b UPR/RNS-E composite

RNS-E can react with the carboxyl and hydroxyl groups of unsaturated polyester chains, thereby forming a local network structure with RNS-E as the network centre. Fig. 8 schematically illustrates the curing process of UPR and UPR/RNS-E composites. A homogeneous cross-linking network structure is formed in cured UPR (Fig. 8*a*), whereas a local network structure is formed in cured UPR/RNS-E composites with the introduction of a proper amount of RNS-E (Fig. 8*b*). This is because RNS-E can directly participate in the polycondensation reaction of UPR to form a heterogeneous structure through strong intermolecular reaction, thereby resulting in a soft interface region with good interfacial adhesion between the RNS-E filler and the polymer matrix. Therefore, the RNS-E, in association with the interfacial region, acts to improve the toughness of the polymer matrix and the transfer stress as well, thereby improving the mechanical properties of the cured UPR/RNS-E composites. When external stresses are applied to cured UPR/RNS-E composites (e.g. during the tensile test and the impact test), the local network structure acts as a stress concentration zone to absorb the external stresses, thereby strengthening and

toughening the polymer matrix. With increase of the RNS-E content, the number of the active centres increases, thus the mechanical properties of the cured UPR/RNS-E composite tend to be improved with increasing RNS-E dosage of up to 0.6%. However, when the content of RNS-E in the composite is above 0.6%, a large amount of the three-dimensional network structure is formed in the cross-linking reaction process of UPR with styrene, which hinders the movement of the polyester chain and reduces the degree of cross-linking reaction of the nanocomposites, thereby worsening the mechanical properties of the cured UPR/RNS-E composites to some extent. As to UPR/RNS-E composites prepared by the mechanical blending process, the local network structure with RNS-E as its centre can hardly be formed, and hence the strengthening effect tends to be worsened as the filler content is above 0.2%.

The SEM images of the impact and tensile fractured surfaces of cured UPR and the *in situ* polymerised UPR/RNS-E composites are shown in Figs. 9 and 10, respectively. It can be seen that the fractured surface of pure UPR (Figs. 9*a* and 10*a*) is relatively smooth and

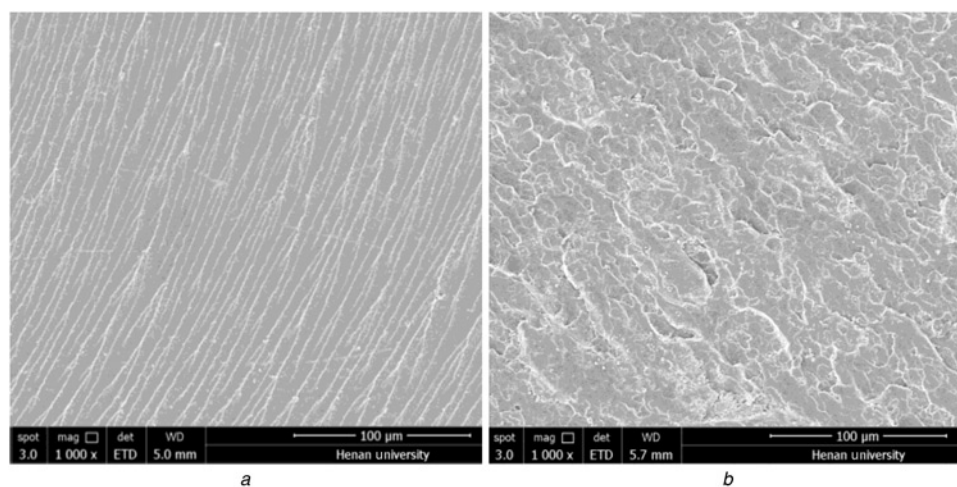


Figure 9 SEM micrographs of impact fractured surfaces of UPR and *in situ* polymerised UPR/RNS-E composite with 0.6% RNS-E

a UPR

b *In situ* polymerised UPR/RNS-E

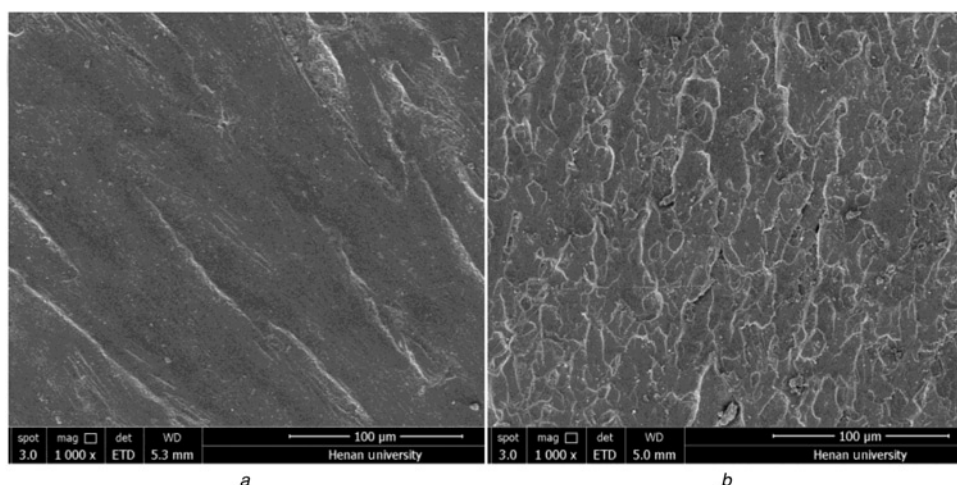


Figure 10 SEM micrographs of tensile fractured surfaces of UPR and *in situ* polymerised UPR/RNS-E

a UPR

b *In situ* polymerised UPR/RNS-E

dominated by the brittle fracture mode, which is because UPR, a typical single-phase glassy material, has poor ability to absorb the external stress. Differing from the pure UPR, the *in situ* polymerised UPR/RNS-E composite with 0.6% RNS-E is dominated by ductile fracture (Figs. 9b and 10b), and cracks on its fractured surface tend to propagate along a tortuous path. This implies that UPR/RNS-E composites subjected to tensile and impact tests are dominated by ductile fracture in association with energy absorption by the inorganic phase and the interfacial zone with the heterogeneous structure.

4. Conclusion: UPR/RNS-E composites have been prepared through *in situ* polycondensation of unsaturated polyester in the presence of the RNS surface capped by the silane coupling agent containing active epoxy group as a reactive monomer. The FT-IR and TGA data prove that RNS-E successfully participates in the polymerisation of unsaturated polyester via an intermolecular cross-linking route, thereby affording UPR/RNS-E composites with the desired interfacial structure and mechanical properties. At an optimal dosage of 0.6%, RNS-E filler can effectively strengthen and toughen the UPR matrix, thereby significantly improving its tensile strength and impact strength. This is because the active epoxy group of the surface capped RNS-E can chemically react with the ester group of the UPR matrix to form a cross-linked heterogeneous network via covalent bonds.

5. Acknowledgment: This research was financially supported by the National Natural Science Foundation of China (grant no. 21371047).

6 References

- Pereira C.M.C., Herrero M., Labajos F.M., Merques A.T., Rives V.: 'Preparation and properties of new flame retardant unsaturated polyester nanocomposites based on layered double hydroxides', *Polym. Degradation Stab.*, 2009, **94**, (6), pp. 939–946
- Ollier R., Rodriguez E., Alvarez V.: 'Unsaturated polyester/bentonite nanocomposites: influence of clay modification on final performance', *Compos. A*, 2013, **48**, pp. 137–143
- Zhang M., Singh R.P.: 'Mechanical reinforcement of unsaturated polyester by Al₂O₃ nanoparticles', *Mater. Lett.*, 2004, **58**, (3), pp. 408–412
- Worzakowska M.: 'Thermal and dynamic mechanical properties of IPNS formed from unsaturated polyester resin and epoxy polyester', *J. Mater. Sci.*, 2009, **15**, (44), pp. 4069–4077
- Chaeichian S., Wood-Adams P.M.: 'In situ polymerization of polyester-based hybrid systems for the preparation of clay nanocomposites', *Polym. J.*, 2013, **54**, (5), pp. 1512–1523
- Yinghong X.: 'Nanometre-sized TiO₂ as applied to the modification of unsaturated polyester resin', *Mater. Chem. Phys.*, 2003, **77**, (2), pp. 609–611
- Feng Y., Wang B., Wang F., ET AL.: 'Thermal degradation mechanism and kinetics of polycarbonate/silica nanocomposites', *Polym. Degradation Stab.*, 2014, **107**, pp. 129–138
- Evora A.V., Shukla A.: 'Fabrication, characterization, and dynamic behavior of polyester/TiO₂ nanocomposites', *Mater. Sci. Eng.*, 2003, **361**, pp. 358–366
- Cai L.F., Lin Z.Y., Qian H.: 'Dispersion of nano-silica in monomer casting nylon6 and its effect on the structure and properties of composites', *Express Polym. Lett.*, 2010, **4**, (7), pp. 397–403
- Zapata P.A., Tamayo L., Pérez M., Cerda E., Azócar I., Rabagliati F. M.: 'Nanocomposites based on polyethylene and nanosilver particles produced by metallocenic 'in situ' polymerization: synthesis, characterization, and antimicrobial behavior', *Eur. Polym. J.*, 2011, (47), pp. 1541–1549
- Chaichana E., Jongsomjit B., Praserttham P.: 'Effect of nano-SiO₂ particle size on the formation of LLDPE/SiO₂ nanocomposite synthesized via the in situ polymerization with metallocene catalyst', *Chem. Eng. Sci.*, 2007, **62**, (3), pp. 899–905
- Goodarzi V., Moremiam S.A., Maleki F., Angaji M.T.: 'In situ radical copolymerization in presence of surface-modified TiO₂ nanoparticles: influence of a double modification on properties of unsaturated polyester (UP) nanocomposites', *J. Macromol. Sci., Phys.*, 2008, **47**, pp. 472–487
- Li X., Cao Z., Zhang Z., Li X.: 'Surface-modification in situ of nano-SiO₂ and its structure and tribological properties', *Appl. Surf. Sci.*, 2006, **252**, (22), pp. 7856–7861
- Shu H., Liu K., Liu F., Zhang Z., Li X.: 'Improving mechanical properties of poly (vinyl chloride) by doping with organically functionalized reactive nanosilica', *J. Appl. Polym. Sci.*, 2013, **129**, (5), pp. 2931–2939
- Zhang J., Guo Z., Zhi X., Tang H.: 'Surface modification of ultrafine precipitated silica with 3-methacryloxypropyltrimethoxysilane in carbonization process', *Colloids Surf. A*, 2013, **418**, pp. 174–179
- Zhang S., Guo M., Chen Z., Liu Q.H., Liu X.: 'Grafting photosensitive polyurethane onto colloidal silica for use in UV-curing polyurethane nanocomposites', *Colloids Surf. A*, 2014, (443), pp. 525–534
- Zhou J., Dong B.: 'A study on the infra-red spectrometry of unsaturated polyesters', *Thermosetting Resin*, 2003, **18**, pp. 22–24
- Ruban Y.J.V., Mon S.G., Roy V.: 'Mechanical and thermal studies of unsaturated polyester-toughened epoxy composites filled with amine-functionalized nanosilica', *Appl. Nanosci.*, 2013, **3**, (1), pp. 7–12
- Liu K., Zheng N., Li X., Zhang Z.: 'Preparation of in-situ surface-modified nanosilica and its application in separating oil from water', *Micro Nano Lett.*, 2013, **1**, (8), pp. 15–18
- Sudirman, Budiarto E., Gunawan I.: 'Synthesis and characterization of polyester-based nanocomposite', *Procedia Chem.*, 2012, (4), pp. 107–113